ICAS 2016
30th Congress of the International Council of the Aeronautical Sciences
DCC, Daejeon, Korea ; September 25-30, 2016

A MESHLESS METHOD FOR SIMULATION OF HYPERSONIC VISCOUS FLOWS

Jin Young Huh*, Jae Sang Rhee*, Kyu Hong Kim, Suk Young Jung*****
***Department of Mechanical & Aerospace Engineering, Seoul National University,**
****Department of Mechanical & Aerospace Engineering/Institute of Advanced Aerospace Technology, Seoul National University,**
*****Agency for Defense Development**

Keywords: *Meshless Method, k-ω SST Turbulence Model, Least Squares Method, AUSMPW+, LU-SGS*

Abstract

This study aims to develop a Meshless (or Gridless) method which can accurately capture strong shock waves in hypersonic viscous flows. Least squares method was used for spatial discretization and AUSMPW+ scheme, a robust and accurate scheme developed to be used for Finite Volume Method(FVM) in hypersonic flows, was modified to be used for Meshless Method. The compressible Reynolds-averaged Navier-Stokes equations with Menter's two equation model are used to describe turbulent flows.
Using the method developed in this study, numerical analyses for hypersonic viscous flows on a flat plate was carried out and the obtained results were compared with those obtained from Structured FVM.

1 Introduction

Generally, grid generation over complex geometry is known to be one of the primary difficulties in computational fluid dynamics. One method to solve this problem is Meshless method. Meshless method does not need rigid domain discretization which can usually be seen as grid form but only needs connectivity information of nodes. In this sense, the more difficult problems tackle, the more concerns of Meshless method arise. In particular, such analysis on hypersonic vehicles often involves multidimensional geometries with leading-edge bluntness and fuselage/wing combinations of arbitrary cross sections.

Many former researchers have studied and developed a number of Meshless methods. For instance, there are Smooth Particle Hydrodynamics method (SPH) which is the first Meshless method, the Element Free Galerkin method, Hp-clouds method, the Reproducing Kernel Particle method, and so on [1]. In compressible fluid dynamics, Sridar [2] and Katz [3] developed Upwind Finite Difference Scheme and Moving Least Squares Method respectively. Also, Huh [4,5] developed Meshless method using AUSMPW+ scheme [6] for inviscid flow, especially for hypersonic flow.

The calculation of aerodynamic forces and heating rates on hypersonic vehicles must take the turbulence into account. For calculation of practical problems on hypersonic fields, the range of flow-field for the Meshless method is improved from invisid flow to turbulent flow. The viscous dissipation term was discretized using least squares method. Menter's k-ω SST turbulence model [7,8] is used to predict the turbulent flow. Results were shown compared with ones from finite volume method.

2 Meshless Method

2.1 Least Squares Method

In the Meshless method, least squares method based on Taylor series expansions has been used to get unknown derivative terms of PDE represented on equation (1).

Ignoring high order terms, the Taylor expansion from the point cloud center (x_0, y_0) is shown as

$$\varphi(x,y) = \varphi_0 + \Delta x \frac{\partial \varphi(x_0)}{\partial x} + \Delta y \frac{\partial \varphi(y_0)}{\partial y} + O(\Delta^2) \qquad (1)$$

The least squares method with weighted function may be expressed as follow

$$min \sum_{j=1}^{n} \omega_{0j} \left[\Delta\varphi_{0j} - \Delta x_{0j} \frac{\partial \varphi(x_0)}{\partial x} - \Delta y_{0j} \frac{\partial \varphi(y_0)}{\partial y} \right]^2 \qquad (2)$$

$$\frac{\partial \varphi}{\partial x} \approx \sum_j a_{0j}(\varphi_j - \varphi_0) \qquad (3)$$

$$\frac{\partial \varphi}{\partial y} \approx \sum_j b_{0j}(\varphi_j - \varphi_0) \qquad (4)$$

For a 2-D case, values of the coefficients are calculated as follow

$$a_{0j} = \frac{\omega_{0j}\Delta x_{0j} \sum \omega \Delta y^2 - \omega_{0j}\Delta y_{0j} \sum \omega \Delta x \Delta y}{\sum \omega \Delta x^2 \sum \omega \Delta y^2 - (\sum \omega \Delta x \Delta y)^2} \qquad (5)$$

$$b_{0j} = \frac{\omega_{0j}\Delta y_{0j} \sum \omega \Delta x^2 - \omega_{0j}\Delta x_{0j} \sum \omega \Delta x \Delta y}{\sum \omega \Delta x^2 \sum \omega \Delta y^2 - (\sum \omega \Delta x \Delta y)^2} \qquad (6)$$

A simple inverse distance weighting function [9] is used to improve accuracy.

$$\omega_{0j} = \frac{1}{(\Delta x_{0j}^2 + \Delta y_{0j}^2)^{1/2}} \qquad (7)$$

2.2 Navier-Stokes Equations and AUSMPW+ for Meshless Method

Consider the 2-D Navier-Stokes equations in strong conservation law form

$$\frac{\partial q}{\partial t} + \frac{\partial f}{\partial x} + \frac{\partial g}{\partial y} = \frac{\partial f_v}{\partial x} + \frac{\partial g_v}{\partial y} \qquad (8)$$

$$q = \begin{bmatrix} \rho \\ \rho u \\ \rho v \\ \rho E \end{bmatrix}, \ f = \begin{bmatrix} \rho u \\ \rho u^2 + P \\ \rho u v \\ \rho u E \end{bmatrix}, \ g = \begin{bmatrix} \rho v \\ \rho u v \\ \rho v^2 + P \\ \rho v E \end{bmatrix}$$
$$f_v = \begin{bmatrix} 0 \\ \tau_{xx} \\ \tau_{xy} \\ -q_x + \phi_x \end{bmatrix}, \ g_v = \begin{bmatrix} 0 \\ \tau_{xy} \\ \tau_{yy} \\ -q_y + \phi_y \end{bmatrix} \qquad (9)$$

where $\phi_i = \tau_{ix} u + \tau_{iy} v$

In Eq. (9), E means the total energy and H means the total enthalpy as follow.

$$E = \frac{P}{(\gamma - 1)\rho} + \frac{1}{2}(u^2 + v^2), \ H = E + \frac{P}{\rho} \qquad (10)$$

Eq. (8) can be discretized as

$$\frac{\partial q_i}{\partial t} + \sum_{j=1}^{n} a_{ij}\Delta f_{ij} + \sum_{j=1}^{n} b_{ij}\Delta g_{ij} = \sum_{j=1}^{n} a_{ij}\Delta f_{v,ij} + \sum_{j=1}^{n} b_{ij}\Delta g_{v,ij}$$
$$\frac{\partial q_i}{\partial t} + \sum_{j=1}^{n} \Delta F_{ij} = \sum_{j=1}^{n} a_{ij}\Delta f_{v,ij} + \sum_{j=1}^{n} b_{ij}\Delta g_{v,ij} \qquad (11)$$

where $F = af + bg$ is a directed flux along the metric weight vector (a, b). To improve accuracy and robustness, AUSMPW+ scheme [6] is applied to the convective term in the N-S equations, which use the midpoint flux at $j + \frac{1}{2}$ instead of the flux at j as follow [3]

$$\sum_{j=1}^{n} \Delta F_{ij} = 2\sum_{j=1}^{n} \Delta F_{ij+\frac{1}{2}} = 2\sum_{j=1}^{n} \left(F_{ij+\frac{1}{2}} - F_{ij}\right) \qquad (12)$$

In Eq. (12), $F_{ij+\frac{1}{2}}$ may be calculated from AUSMPW+ scheme.

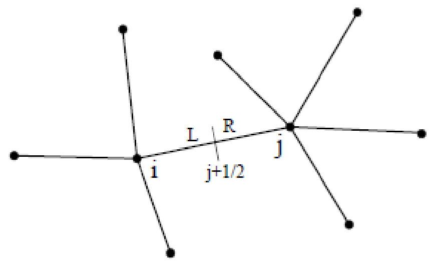

Fig. 1. Illustration of mid-point value on the edge connecting nodes i and j

The numerical flux of AUSMPW+ is given by

$$F_{\frac{1}{2}} = \bar{M}^{+}{}_{L} c_{\frac{1}{2}} \Phi_L + \bar{M}^{-}{}_{R} c_{\frac{1}{2}} \Phi_R + (P_L^+ P_L + P_R^- P_R) \qquad (13)$$

$\Phi = (\rho, \rho u, \rho H)^T$ and $P = (0, p, 0)^T$. The subscripts 1/2 and (L,R) stand for a quantity at a midpoint on the edge of Fig. 1 and the left and right states across the edge, respectively. The Mach number at midpoint is defined as

$$m_{\frac{1}{2}} = M_L^+ + M_R^- \qquad (14)$$

when $\overline{M_L^+}$ and $\overline{M_R^-}$ are given as follow.

If $m_{\frac{1}{2}} = M_L^+ + M_R^- \geq 0$, then

$$\overline{M_L^+} = M_L^+ + M_R^-[(1-w)(1+f_R) - f_L] \qquad (15)$$

$$\overline{M_R^-} = M_R^- w(1+f_R) \quad (16)$$

If $m_{\frac{1}{2}} = M_L^+ + M_R^- < 0$, then

$$\overline{M_L^+} = M_L^+ + w(1+f_L) \quad (17)$$

$$\overline{M_R^-} = M_R^- + M_L^+[(1-w)(1+f_L) - f_R] \quad (18)$$

with

$$w(P_L, P_R) = 1 - min\left(\frac{P_L}{P_R}, \frac{P_R}{P_L}\right)^3 \quad (19)$$

The pressure-based weight function is simplified to

$$f_{L,R} = \left(\frac{P_{L,R}}{P_s} - 1\right), P_s \neq 0 \quad (20)$$

where

$$P_s = P_L^+ P_L + P_R^- P_R \quad (21)$$

The split Mach number is defined by

$$M^{\pm} = \begin{cases} \pm\frac{1}{4}(M \pm 1)^2, & |M| \leq 1 \\ \frac{1}{2}(M \pm |M|), & |M| > 1 \end{cases} \quad (22)$$

$$P^{\pm} = \begin{cases} \frac{1}{4}(M \pm 1)^2(2 \mp M), & |M| \leq 1 \\ \frac{1}{2}(1 \pm sign(M)), & |M| > 1 \end{cases} \quad (23)$$

The Mach number of each side is

$$M_{L,R} = \frac{U_{L,R}}{c_{1/2}} \quad (24)$$

and the speed of sound($c_{1/2}$) is

$$c_{1/2} = \begin{cases} min\left(\frac{c^{*2}}{max(|U_L|, c^*)}\right), \frac{1}{2}(U_L + U_R) > 0 \\ min\left(\frac{c^{*2}}{max(|U_R|, c^*)}\right), \frac{1}{2}(U_L + U_R) < 0 \end{cases} \quad (25)$$

where

$$c^* = \sqrt{2(\gamma - 1)/(\gamma + 1)H_{normal}} \quad (26)$$

$$H_{normal} = \frac{1}{2}(H_L - \frac{1}{2}V_L^2 + H_R - \frac{1}{2}V_R^2) \quad (27)$$

2.3 Minmod Limiter for Meshless Method

To improve accuracy, TVD scheme is adopted to the Meshless method. In this study, minmod limiter [4] is used at AUSMPW+. The basic form of spatial interpolation is given by

$$\Phi_L = \Phi_i + 0.5 * \phi_L * (\Phi_j - \Phi_i)$$
$$\Phi_R = \Phi_j + 0.5 * \phi_R * (\Phi_i - \Phi_j) \quad (28)$$

In order to apply to Meshless method, it is necessary to modify minmod limiter as follows. In Meshless method, ϕ is given by

$$\phi = max(0, min(1, r_k)), \quad (29)$$

where $k \in \{local\ point\ cloud\ of\ node\ i\ \&\ \theta_{kij}\ is\ max\}$,

$$r_k = \frac{s_{ik'}}{s_{ji}} = \frac{s_{ki}}{s_{ji}} cos(\theta_{kij}), \quad (30)$$

$$s_{ki} = \frac{\Phi_k - \Phi_i}{\|\overrightarrow{x_k} - \overrightarrow{x_i}\|} \quad (31)$$

Since there is no point on the opposite side of point j in the vicinity of point i in general point system, nearest point k to the opposite side is used to calculate r_k as shown in Fig. 2.

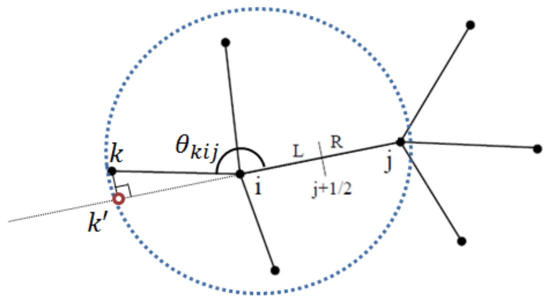

Fig. 2. Minmod limiter for Meshless method

3 Application of the Meshless Method to the Reynolds-Averaged Navier-Stokes Equations

For a turbulent flow, the Reynolds-averaged Navier-Stokes equations are used. Menter's k-ω SST model [7,8] is written as follows

$$\frac{\partial(\rho k)}{\partial t} + \frac{\partial(\rho u k)}{\partial x} + \frac{\partial(\rho v k)}{\partial y} = P - \beta^* \rho \omega k$$
$$+ \frac{\partial}{\partial x}\left[(\mu + \sigma_k \mu_t)\frac{\partial k}{\partial x}\right] + \frac{\partial}{\partial y}\left[(\mu + \sigma_k \mu_t)\frac{\partial k}{\partial y}\right] \quad (32)$$

$$\frac{\partial(\rho \omega)}{\partial t} + \frac{\partial(\rho u \omega)}{\partial x} + \frac{\partial(\rho v \omega)}{\partial y} = \frac{\gamma}{\nu_t} P - \beta \rho \omega^2$$
$$+ \frac{\partial}{\partial x}\left[(\mu + \sigma_\omega \mu_t)\frac{\partial \omega}{\partial x}\right] + \frac{\partial}{\partial y}\left[(\mu + \sigma_\omega \mu_t)\frac{\partial \omega}{\partial y}\right] \quad (33)$$

$$+2(1-F_1)\frac{\rho\sigma_{\omega 2}}{\omega}\left(\frac{\partial k}{\partial x}\frac{\partial \omega}{\partial x}+\frac{\partial k}{\partial y}\frac{\partial \omega}{\partial y}\right)$$

Production term is given by:

$$P=\min\left(\tau_{ij}\frac{\partial u_i}{\partial x_j},20\beta^*\rho\omega k\right) \tag{34}$$

$$\tau_{ij}=\mu_t\left(2S_{ij}-\frac{2}{3}\frac{\partial u_k}{\partial x_k}\delta_{ij}\right)-\frac{2}{3}\rho k\delta_{ij} \tag{35}$$

$$S_{ij}=\frac{1}{2}\left(\frac{\partial u_i}{\partial x_j}+\frac{\partial u_j}{\partial x_i}\right) \tag{36}$$

and the turbulent eddy viscosity is given by:

$$\mu_t=\frac{\rho a_1 k}{\max(a_1\omega,\Omega F_2)} \tag{37}$$

Each of the constants is a blend of an inner and outer constant.

$$\phi=F_1\phi_1+(1-F_1)\phi_2 \tag{38}$$

where ϕ_1 represents an inner constant and ϕ_1 represents an outer constant. Additional functions are defined by:

$$F_1=\tanh(\arg_1^4) \tag{39}$$

$$arg_1=\min\left[\max\left(\frac{\sqrt{k}}{\beta^*\omega d},\frac{500\nu}{d^2\omega}\right),\frac{4\rho\sigma_{\omega 2}k}{CD_{k\omega}d^2}\right] \tag{40}$$

$$CD_{k\omega}=max\left[2\rho\sigma_{\omega 2}\frac{1}{\omega}\frac{\partial k}{\partial x_j}\frac{\partial \omega}{\partial x_j},10^{-20}\right] \tag{41}$$

$$F_2=tanh(arg_2^2) \tag{42}$$

$$arg_2=max\left(2\frac{\sqrt{k}}{\beta^*\omega d},\frac{500\nu}{d^2\omega}\right) \tag{43}$$

$$\Omega=\sqrt{2W_{ij}W_{ij}} \tag{44}$$

$$W_{ij}=\frac{1}{2}\left(\frac{\partial u_i}{\partial x_j}-\frac{\partial u_j}{\partial x_i}\right) \tag{45}$$

The constants are given by:

$$\gamma_1=\frac{\beta_1}{\beta^*}-\frac{\sigma_{\omega 1}\kappa^2}{\sqrt{\beta^*}},\quad \gamma_2=\frac{\beta_2}{\beta^*}-\frac{\sigma_{\omega 2}\kappa^2}{\sqrt{\beta^*}}$$

$$\sigma_{k1}=0.85,\sigma_{\omega 1}=0.5,\beta_1=0.075 \tag{46}$$

$$\sigma_{k2}=1.0,\sigma_{\omega 2}=0.856,\beta_2=0.0828$$

$$\beta^*=0.09,\kappa=0.41,a_1=0.31$$

Eq. (32) and (33) are also discretized like Eq. (11).

4 LU-SGS for Meshless Method

Referring to the works of Yoon [10] and Chen [11], LU-SGS is adopted to Meshless Method. By applying Eq. (11) and (12), the governing equation (8) and can be rewritten in a semi-discrete form as follows

$$\frac{\partial q_i^{n+1}}{\partial t}+2\sum_{j=1}^{n}(F_{ij}^{n+1}-F_i^{n+1})=\sum_{j=1}^{n}(a_{ij}\Delta f_{v,ij}^n+b_{ij}\Delta g_{v,ij}^n) \tag{47}$$

The flux function, F_{ij}^{n+1} may be linearized by setting

$$F_{ij}^{n+1}(\omega_i,\omega_j)\approx F_{ij}^n+A_{ij}^+(\omega_i)\delta\omega_i+A_{ij}^-(\omega_j)\delta\omega_j \tag{48}$$

where n is the time level and matrices $A_{ij}^{\pm}$ are constructed as follow

$$A_{ij}^{\pm}=\frac{1}{2}(A_{ij}\pm\lambda_{ij}I) \tag{49}$$

where

$$\lambda_{ij}\geq\max(|\lambda_A|) \tag{50}$$

Here, λ_A represents eigenvalues of Jacobian matrix.

5 Numerical Result

In order to verify the Meshless method, flow over a flat plate has been chosen as a hypersonic test case to illustrate the behavior of the laminar/turbulent flow results obtained using both Meshless method and finite volume method (FVM) with structured grid system. The numerical schemes and flow conditions used are tabulated as Table 1. The free stream conditions are at altitude 15km and the schematic of flow geometry is shown in Fig.3. [12]

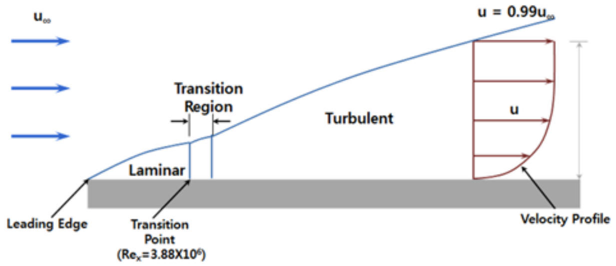

Fig. 3. Schematic of the flat plate

Table 1. Schemes and flow conditions

Computational method	Meshless, structured FVM
Spatial discretization	AUSMPW+
Limiter	Minmod
Time integration	LU-SGS
Freestream Flow Conditions	$p_\infty = 1.21114 \times 10^4 N/m^2$, $T_\infty = 216.65\ K$ $M_\infty = 8$ $\mu_\infty = 1.4216 \times 10^{-5} N \cdot s/m^2$
Number of Points	13,041

The Meshless method and FVM both used AUSMPW+. The point system for validation is shown in Fig. 3 and the same point distribution was applied to the both method. Fig. 4 shows the skin friction coefficients along Re_x obtained by the developed method and FVM and its results are compared to the accurate laminar and turbulent results obtained for this case by Van Driest[13,14]. The transition location was specified at $Re_x = 3.88 \times 10^6 (x = 0 .1196\ m)$. It has been observed that the result of the Meshless method predict skin friction in both laminar and turbulent region in agreement with the theory.

Convergence history of Meshless method and FVM, which is L_2 norms of the residuals for density, is presented in Fig. 5. The figure shows the both method has good convergence characteristics.

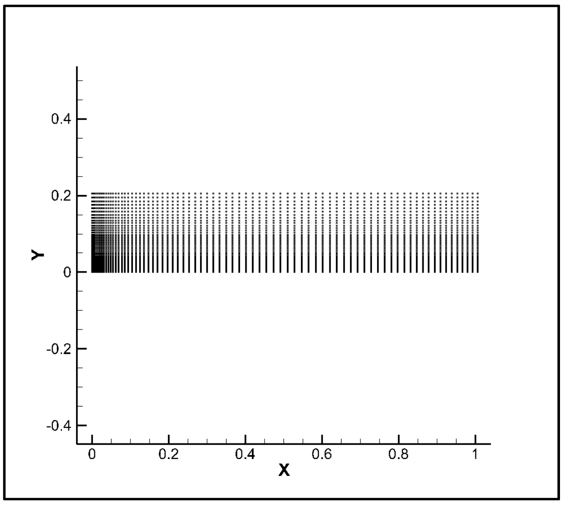

Fig. 4. Computational domain (13,041 points)

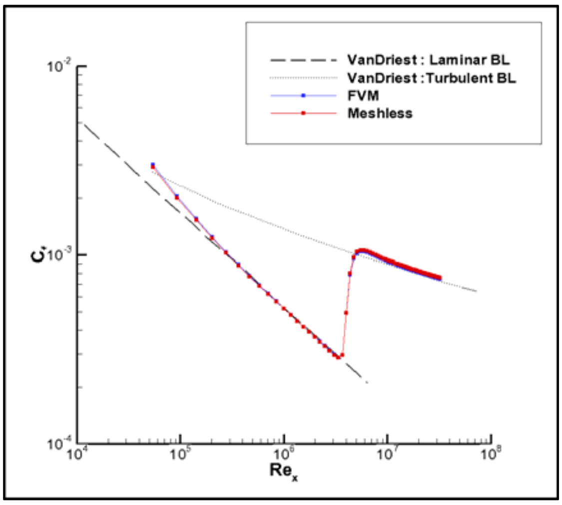

Fig. 5. Skin friction coefficients comparison

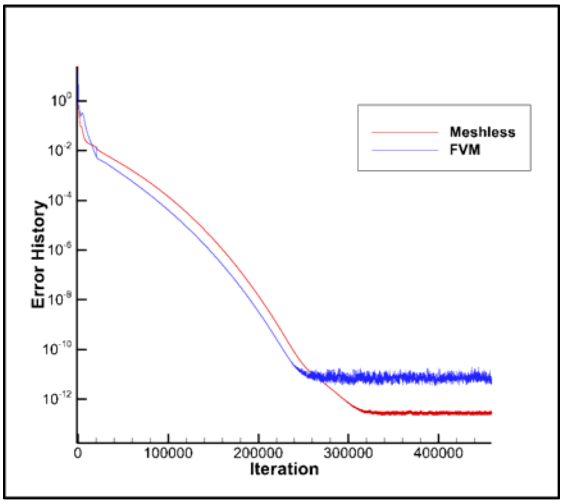

Fig. 6. Comparisons of convergence histories

6 Conclusion

The purpose of this study is to develop Meshless method for hypersonic viscous flows. A least squares method was used for spatial discretization and AUSMPW+ scheme and LU-SGS was modified to be used for Meshless Method. Menter's k-ω SST model is chosen as turbulence model. According to the comparison of analyses of the numerical results, Meshless method was confirmed to have similar accuracy and convergence as structured finite volume method.

References

[1] Liu G R. *Mesh Free Methods: Moving Beyond the Finite Element Method,* CRC Press, 2003.

[2] Sridar D and Balakrishnan N. An upwind finite difference scheme for meshless solvers, *J. Comput. Phys.*, Vol. 189, pp 1-29, 2003.

[3] Katz A and Jameson A. A Comparison of Various Meshless Schemes Within a Unified Algorithm, AIAA 2009-596, *47th AIAA Aerospace Sciences Meeting Including The New Horizons Forum and Aerospace Exposition*, Orlando, Florida, 2009.

[4] Huh J, Kim K and Jung S. Meshless Method for Simulation of 2-D Compressible Flow, *The 2013 Asia-Pacific International Symposium on Aerospace Technology*, Takamatsu, Japan, 2013.

[5] Huh J, Kim K and Jung S. Meshless Method for Simulation of Compressible Reacting Flow, *29th Congress of the International Council of the Aeronautical Sciences*, Russia, 2014.

[6] Kim K, Kim C and Rho O. Methods for the Accurate Computations of Hypersonic Flows I. AUSMPW+ Scheme, *Journal of Computational Physics*, Vol.174, pp 38-80, 2001.

[7] Menter F R. Two-Equation Eddy-Viscosity Turbulence Models for Engineering Applications, *AIAA Journal,* Vol. 32, No. 8, pp 1598-1605, 1994.

[8] Menter F R and Kuntz M Langtry R. Ten years of industrial experience with the SST model, Turbulence, Heat and Mass Transfer 4, vol. 4, pp. 625-632, 2003.

[9] Mavriplis D J. Revisiting the least-squares procedure for gradient reconstruction on unstructured meshes, AIAA paper 2003-3986, *AIAA 16th Computational Fluid Dynamics Conference*, 2003.

[10] Yoon S and Jameson A. Lower-Upper Symmetric-Gauss-Seidel Method for the Euler and Navier-Stokes Equations, *AIAA Journal*, Vol. 26, No. 9, pp 1025-1026, 1988.

[11] Chen H Q and Shu C. An Efficient Implicit Mesh-Free Method To Solve Two-Dimensional Compressible Euler Equations, *International Journal of Modern Physics C.,* Vol. 16, No. 3, pp 439-454, 2005.

[12] Christopher J. Roy, Frederick G. Blottner, Methodology for Turbulence Model Validation : Application to Hypersonic Flows, *Journal of spacecraft and rockets*, Vol. 40, No. 3, 2003.

[13] Van Driest E R. Investigation of Laminar Boundary Layer in Compressible Fluids Using the Crocco Method, *National Advisory Committee for Aeronautics*, NACA TN-2597, 1952.

[14] Van Driest E R. Problem of Aerodynamic Heating, *Aeronautical Engineering Review*, Vol. 15, No. 10, pp 26-41, 1956.

Acknowledgments

- This research was supported by Space Core Technology Program through the National Research Foundation of Korea(NRF) funded by the Ministry of Science, ICT & Future Planning(NRF-2015M1A3A3A05027630)
- This work was supported by the Brain Korea 21 Plus Project in 2016

Contact Author Email Address

Mailto:aerocfd1@snu.ac.kr

Copyright Statement